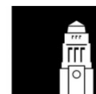

UNIVERSITY OF LEEDS

This is a repository copy of *Modulating in vitro gastric digestion of emulsions using composite whey protein–cellulose nanocrystal interfaces*.

White Rose Research Online URL for this paper:
http://eprints.whiterose.ac.uk/118424/

Version: Accepted Version

Article:

Sarkar, A orcid.org/0000-0003-1742-2122, Zhang, S, Murray, B orcid.org/0000-0002-6493-1547 et al. (2 more authors) (2017) Modulating in vitro gastric digestion of emulsions using composite whey protein–cellulose nanocrystal interfaces. Colloids and Surfaces B: Biointerfaces, 158. pp. 137-146. ISSN 0927-7765

https://doi.org/10.1016/j.colsurfb.2017.06.037

(c) 2017, Elsevier B.V. This manuscript version is made available under the CC BY-NC-ND 4.0 license http://creativecommons.org/licenses/by-nc-nd/4.0/

Reuse
Items deposited in White Rose Research Online are protected by copyright, with all rights reserved unless indicated otherwise. They may be downloaded and/or printed for private study, or other acts as permitted by national copyright laws. The publisher or other rights holders may allow further reproduction and re-use of the full text version. This is indicated by the licence information on the White Rose Research Online record for the item.

Takedown
If you consider content in White Rose Research Online to be in breach of UK law, please notify us by emailing eprints@whiterose.ac.uk including the URL of the record and the reason for the withdrawal request.

eprints@whiterose.ac.uk
https://eprints.whiterose.ac.uk/

Modulating in vitro gastric digestion of emulsions using composite whey protein–cellulose nanocrystal interfaces

Anwesha Sarkar [1]*, Shuning Zhang [1], Brent Murray [1], Jessica A. Russell [1] and Sally Boxal [2]

[1] Food Colloids and Processing Group, School of Food Science and Nutrition, University of Leeds, Leeds LS2 9JT, UK

[2] Bioimaging Facility, Faculty of Biological Sciences, University of Leeds, Leeds LS2 9JT, UK

Total number of words: 5883

Number of Figures: 6

Number of Tables: 2

*Corresponding author:

Dr. Anwesha Sarkar

Food Colloids and Processing Group,

School of Food Science and Nutrition, University of Leeds, Leeds LS2 9JT, UK.

E-mail address: A.Sarkar@leeds.ac.uk (A. Sarkar).

Tel.: +44 (0) 113 3432748.

Abstract

In this study, we designed emulsions with an oil-water interface consisting of a composite layer of whey protein isolate (WPI, 1 wt%) and cellulose nanocrystals (CNCs) (1-3 wt%). The hypothesis was that a secondary layer of CNCs at the WPI-stabilized oil-water interface could protect the interfacial protein layer against in vitro gastric digestion by pepsin at 37 ^{0}C. A combination of transmission electron microscopy, ζ-potential measurements, interfacial shear viscosity measurements and theoretical surface coverage considerations suggested the presence of CNCs and WPI together at the O/W interface, owing to the electrostatic attraction between complementarily charged WPI and CNCs at pH 3. Microstructural analysis and droplet sizing revealed that the presence of CNCs increased the resistance of the interfacial protein film to rupture by pepsin, thus inhibiting droplet coalescence in the gastric phase, which occurs rapidly in an emulsion stabilized by WPI alone. It appeared that there was an optimum concentration of CNCs at the interface for such barrier effects. Sodium dodecyl sulphate polyacrylamide gel electrophoresis (SDS-PAGE) results further confirmed that the presence of 3 wt% of CNCs reduced the rate and extent of proteolysis of protein at the interface. Besides, evidence of adsorption of CNCs to the protein-coated droplets to form more rigid layers, there is also the possibility that network formation by the CNCs in the bulk (continuous) phase reduced the kinetics of proteolysis. Nevertheless, structuring emulsions with mixed protein-particle layers could be an effective strategy to tune and control interfacial barrier properties during gastric passage of emulsions.

Keywords

Cellulose nanocrystals, emulsion; in vitro gastric digestion; particle-protein interface; whey protein; pepsin

1 Introduction

Emulsions stabilized by biopolymer-based particles, such as those derived from proteins [1-4] and polysaccharides [5-7] have attracted a lot of attention recently owing to the demand for ultra-stable emulsions and biocompatible 'clean-label' emulsifiers that are immediately suitable for use in food, pharmaceutical, cosmetics, and other allied soft matter applications [8-10]. Besides their unique interfacial stabilizing properties, particles, such as whey protein microgel particles [2] and chitin [11] have also shown abilities to modulate digestion of emulsified lipids by restricting the access of lipase to the hydrophobic lipid substrate. Such lipid digestion modulating properties might be exploited to enhance satiety or used for targeted release of bioactive components within the gastrointestinal tract [2, 11-16].

However, it is worth recognizing that biochemical processes occurring in the gastric regime might hinder such impact owing to the hydrolysis of the Pickering stabilizers by pepsin, as previously reported for protein-based particles [2, 17]. Such rupture of the interfacial particle layers may induce gastric instability, such as flocculation and coalescence [2, 18-20]. In view of such possible gastric destabilization studies, it might be useful to create a much more complex interface to help protect the emulsions against pepsin attack. In this regard, cellulose nanocrystals (CNCs) are interesting candidates for creating an interfacial barrier surrounding the protein interface, since human enzymes cannot digest cellulose.

Solid rod-like cellulose nanocrystals (CNCs) derived from world's most abundant biopolymer are a biocompatible and renewable source material. They are typically 5–70 nm in width and between 100 nm and several micrometers in lengths [21]. Biopolymer-based particles derived from proteins are intrinsically surface-active, but most CNCs, widely manufactured via sulphuric acid treatment, create

75 strong sulphate charges on the CNC particles, increasing their hydrophilicity so that
76 they are not wetted by oil unless chemically modified [12, 22], i.e. their surface
77 activity is low.

78 In this study, we utilized the negative charge on CNCs to create composite
79 WPI + CNCs interfaces at pH 3. The hypothesis was that the presence of unmodified
80 CNCs at the WPI-stabilized O/W interface could enhance the gastric stability of the
81 corresponding emulsions by acting as a barrier to the pepsin attacking the whey
82 protein at the interface. Although there have already been recent reports of mixed
83 protein-polysaccharide particle interfaces, such as chitin nanocrystals + *β*-
84 lactoglobulin [23], cellulose particles + sodium caseinate [24], to our knowledge, this
85 is the first study that reports the effect of combining whey protein + unmodified CNC
86 particles synergistically at interface and discover the influence of such composite
87 layers on enhanced gastric stability in a simulated gastric condition. The properties of
88 freshly prepared emulsions and pepsin-digested emulsions were measured using
89 particle sizing, microscopy at various length scales (confocal laser scanning
90 microscopy, transmission electron microscopy), SDS PAGE (sodium dodecyl
91 sulphate polyacrylamide gel electrophoresis) analysis, *ζ*-potential and interfacial shear
92 viscosity measurements.
93

94 **2 Materials and Methods**

95 2.1 Materials

96 Cellulose nanocrystal powder (CNCs) was purchased from CelluForce™, Canada
97 According to the manufacturer; it contained of 100% sulphated CNCs. Whey protein
98 isolate (WPI) powder containing 96.3 wt% protein was kindly gifted by Fonterra
99 Limited (Auckland, New Zealand). Microcrystalline cellulose (MCC), produced by

100 acid hydrolysis of cellulose, product code 310697 and pure β-lactoglobulin (β-lg), ≥
101 90% (PAGE), product code L3908, were purchased from Sigma Aldrich, (New Jersey
102 USA). Sunflower oil was purchased from a local supermarket (Morrisons, UK).
103 Pepsin enzyme (P7000-25G, actual activity: 474 U mg^{-1}) was purchased from Sigma-
104 Aldrich Company Ltd, Dorset, UK. All other chemicals used were of analytical grade
105 unless otherwise specified. Mini-Protean Precast TGX Gels (8-16%) and Precision
106 Plus Protein All Blue Standards were purchased from Bio-Rad Laboratories, Inc,
107 USA. Milli-Q water having an ionic purity of 18.2 MΩ·cm at 25 °C (water purified
108 by treatment with a Milli-Q apparatus) was used for all the experiments.

109

110 2.2 Preparation of emulsions

111 Oil-in-water emulsions stabilized by WPI and/or CNCs were prepared with 10 mM
112 citrate buffer solution at pH 3 (adjusted using 0.1 M HCl). Whey protein isolate
113 (WPI) solution was prepared by dispersing appropriate quantities of WPI in citrate
114 buffer and stirring for 2 h at room temperature to ensure complete dissolution of the
115 protein. Oil-in-water emulsions (20 wt% oil) stabilized by WPI (1 wt%), hereafter
116 reported as W1 were prepared by homogenizing 20.0 wt% sunflower oil and 80.0
117 wt% WPI solution using a Leeds Jet Homogenizer at 300 bar pressure at 25 °C. For
118 preparing the protein-particle-stabilized interfaces. primary emulsions (40 wt% oil)
119 were prepared first using WPI by passing through the Jet Homogenizer. Secondary
120 emulsions were prepared by dispersing the primary emulsions into CNCs dispersions
121 (2-6 wt% in citrate buffer at pH 3) (1:1 w/w) to achieve final concentration of 20 wt%
122 oil, 1 wt% WPI and 1 or 3 wt% CNCs, hereafter cited as W1C1 or W1C3,
123 respectively. Sodium azide (0.02 wt%) was added to the emulsions to prevent
124 microbial growth during refrigerated storage at 4 °C.

125 2.3 Particle size analysis of emulsions

126 A Malvern MasterSizer 3000 (Malvern Instruments Ltd, Malvern, Worcestershire,
127 UK) was used to measure the droplet size distribution of each of the three emulsions
128 before and after gastric digestion. The relative refractive index, i.e., the ratio of
129 sunflower oil (1.456) to that of dispersion medium (1.33) was 1.095. Droplet size
130 measurements were reported as Sauter-average diameter (d_{32}) and volume-average
131 diameter (d_{43}) from the particle size distributions, using equations 1 and 2,
132 respectively:

133

134–135
$$d_{32} = \frac{n_i d_i^3}{n_i d_i^2} \tag{1}$$

136

137–138
$$d_{43} = \frac{n_i d_i^4}{n_i d_i^3} \tag{2}$$

139

140 where, n_i is the number of particles with diameter d_i. Mean and standard deviations
141 were calculated on five measurements on triplicate samples.

142

143 2.4 Interfacial shear viscosity (η_i)

144 Simple measurements of interfacial shear rheology at pH 3 were used to test for the
145 presence of attractive interactions between anionic cellulose and whey proteins.
146 Interfacial shear rheology is particularly sensitive to the composition of and
147 interactions at an interface [25, 26]. In addition, interfacial shear viscosity (η_i) has
148 been shown to be sensitive to the accumulation of particles at interfaces in the
149 presence of protein. For example, authors [27] have demonstrated a significant

150 increase in η_i at the air-water interface in the presence of stable O/W emulsion
151 droplets when sodium caseinate was also adsorbed, whilst even larger increases in η_i
152 were seen [28] in the presence of hydrophobically modified cellulose and starch
153 granule particles. Safouane, Langevin & Binks (2007) [29] have reported extremely
154 stiff films of partially hydrophobic particles at the air-water interface.

155 Because the CNC sample from CelluForce™ used in this study was relatively
156 expensive and the supply very limited, we chose to use the MCC sample since this
157 was relatively cheap and readily available. As described in the Results and
158 Discussion section, the MCC and the CNC are expected to have similar zeta potentials
159 and aspect ratio (as derived from optical micrograph) as a function of pH. A two
160 dimensional Couette-type interfacial viscometer [26], was operated in a constant
161 shear-rate mode, as described in recent studies [27, 30]. Briefly, a stainless steel
162 biconical disc (radius 14.5 mm) was suspended from a thin torsion wire with its edge
163 in the plane of the air-water (A–W) or oil-water (O–W) interface of the solution
164 contained within a cylindrical glass dish (radius 72.5 mm). The constant shear rate
165 apparent interfacial viscosity, η_i, is given by the following equation:

166 $$\eta_i = \frac{g_f}{\omega} K(\theta - \theta_0) \tag{3}$$

167 where K is the torsion constant of the wire; θ is the equilibrium deflection of the disc
168 in the presence of the film; θ_0 is the equilibrium deflection in the absence of the film,
169 i.e., due to the bulk drag of the sub-phase on the disc; g_f is the geometric factor and ω
170 is the angular velocity of the dish. A fixed value of $\omega = 1.27 \times 10^{-3}$ rad s^{-1} was
171 employed throughout, for comparison with previous measurements of proteins +
172 particles [28]. For experiments at the O–W interface, a layer of pure n-tetradecane
173 was layered over the aqueous solution within 1 min of adding the aqueous phase to

174 the dish. Pure β-lg at a concentration of 10^{-3} wt% was used as the aqueous phase,
175 representative of the main component of WPI and again for comparison with previous
176 measurements with hydrophobically modified cellulose, with or without added MCC
177 (1 wt% or 3 wt%) at pH 3 or 7. Experiments were repeated at least three times and
178 the η_i results are reported as the mean values ± the range about the mean.
179
180 ## 2.5 Zeta-potential
181 A Zetasizer Nano ZS (Malvern Instruments Ltd, Malvern, Worcestershire, UK) was
182 used to measure the ζ-potential of each of the emulsions before and after gastric
183 digestion (120 minutes). Emulsions were diluted to 0.005 wt% droplet concentration
184 and the solution was transferred into a DTS1070 folded capillary to measure the
185 electrophoretic mobility, which was converted to ζ-potential using classical
186 Smoluchowski equation. Each individual ζ-potential data point was reported as the
187 average and standard deviation of at least five reported readings made on triplicate
188 samples.
189
190 ## 2.6 Transmission electron microscopy (TEM)
191 Transmission electron microscopy (TEM) was employed to observe the structure of
192 the CNCs and the original emulsions. Samples (10 µL) were fixed with 2.5% (v/v)
193 glutaraldehyde and post fixed in 0.1% (w/v) osmium tetroxide 32. Then, the samples
194 were subjected to serial dehydration in ethanol (20-100%) before being embedded in
195 araldite. Ultra-thin sections (silver-gold 80-100 nm) were deposited on 3.05 mm grids
196 and stained with 8% (v/v) uranyl acetate and lead citrate. The sections were cut on an
197 "Ultra-cut" microtome. Images were recorded using a CM10 TEM microscope
198 (Philips, Surrey, UK).

199 2.7 Confocal laser scanning microscopy (CLSM)

200 Confocal laser scanning microscopy (CLSM) of the emulsions before and after in
201 vitro gastric digestion were imaged using a Zeiss LSM 880 confocal microscope (Carl
202 Zeiss MicroImaging GmbH, Jena, Germany). Nile Red was used to stain oil
203 (Excitation 514 nm, Emission 539-648 nm), Fast Green was used to stain WPI
204 (Excitation 633 nm, Emission 657-755 nm) and Calcofluor White was used to stain
205 CNCs (Excitation 405 nm, Emission 410-523 nm). A small quantity of emulsion
206 before and immediately after gastric digestion (30 min, 120 min) was placed on a
207 concave microscope slide. About 10 μL each of Nile Red (0.1% w/v in dimethyl
208 sufoxide), Fast Green (0.1% w/v in Milli Q water) and Calcofluor White (0.1% w/v in
209 Milli Q water) was added to the samples and stained for 30 min. Finally, the sample
210 was covered with a cover slip and imaged using a 63× magnification oil immersion
211 objective lens.

212

213 2.8 In vitro gastric digestion

214 Emulsions were digested by mixing them with simulated gastric fluid (SGF) with
215 pepsin using the harmonized digestion protocol (Minekus et al., 2014) at 37 °C.
216 Briefly, 20 mL of the emulsions (20 wt% oil) were incubated for 2 hours in 20 mL of
217 SGF, which consisted of 0.514 g L^{-1} KCl, 0.123 g L^{-1} KH_2PO_4, 0.042 g L^{-1} $NaHCO_3$,
218 0.06 g L^{-1} NaCl, 0.0004 g L^{-1} $MgCl_2(H_2O)_6$, 0.0009 g L^{-1} $(NH_4)_2CO_3$ and 3.2 g L^{-1}
219 pepsin. The pH value of SGF was adjusted to pH 3 using 0.1 M HCl to simulate after
220 meal ingestion conditions. To observe the change of emulsions during digestion,
221 aliquots were collected at different time intervals between 0 and 120 min for analysis.

222

223

2.9 SDS-PAGE (sodium dodecyl sulphate polyacrylamide gel electrophoresis)

To determine the influence of CNCs on digestion of the adsorbed WPI at the O/W interface, the cream phase of W1, W1C1 and W1C3 emulsions sampled at various time intervals during in vitro gastric digestion was analysed using sodium dodecyl sulphate polyacrylamide gel electrophoresis (SDS-PAGE). Samples (1 mL) were heated at 95 °C for 5-10 min to stop digestion. Control experiments were also carried out where pepsin activity was stopped in the three emulsions by raising the pH to pH 7 using 0.5 M ammonium bicarbonate from 0-60 minutes and then using 0.1 N NaOH after 60 min. The aliquots were centrifuged for 40 min at 14500g and 20 °C using a table-top micro-centrifuge (Eppendorf MiniSpin plus, Scientific Laboratory Supplies. Ltd. UK). A certain amount of cream layer was carefully collected, mixed with 50 µL SDS buffer (1 M Tris, pH 6.8) and again heated at 95 °C for 5-10 min. The SDS-PAGE was carried out by loading 5 µL of protein marker and 10 µL of digested samples + loading buffer mixtures into precast gels, then placed in Mini-PROTEAN II system (Bio-Rad Laboratories, Inc, USA). The running process had two stages: 100 V for 10 min followed by 200 V for 20 min. The gels were then stained for 2 hours with 90 wt% ProtoBlue Safe Colloidal Coomassie G-250 stain and 10 wt% ethanol. After staining, the gels were destained using distilled water overnight and then scanned using a ChemiDoc™ XRS+ system with image LabTM Software (Bio- Rad Laboratories, Inc, USA). The SDS-PAGE experiments were repeated three times.

2.10 Statistical analysis

The results were statistically analyzed by analysis of variance (ANOVA) with Tukey's post-hoc test using Graphpad 5 Prism software and differences were considered significant when $p<0.05$ were obtained.

250 **Results and discussion**

251 Firstly, CNCs were charcaterized in order to understand better the properties of the
252 emulsions stabilized by protein plus CNCs. The secondary coverage of protein-
253 stabilized interface by different concentrations of CNCs was calculated. The
254 behaviour of these emulsions (W1, W1C1 and W1C3) during in vitro gastric digestion
255 conditions was then assessed.

256

257 3.1 Characteristics of CNC and MCC

258 The TEM image (Figure 1) suggests that the CNCs were stiff, needle-like particles of
259 a nearly perfect crystalline structure with a diameter of ~ 100 nm, very similar to
260 those reported by Scheuble, et al., 2016 using atomic force microscopy images [12].
261 A percolated network-type architecture was observed at 3 wt% CNC (Figure 1A).
262 This is expected due to the high aspect ratio of CNCs, i.e. the ratio of length to
263 diameter (L/D), which was within the range of 10 to 50 (Figure 1B), consistent with
264 previous reports [31]. Dispersions of CNCs at 1 and 3 wt% were anionic at pH 3 with
265 ζ-potential values of –39.6 and –43.8 mV, respectively (data not shown). Such
266 negative charge has been attributed to processing conditions using sulphuric acid
267 hydrolysis resulting in negatively charged sulphate groups grafted to the surface of the
268 individual cellulose chains [31].

269 The nominal particle size of the MMC cellulose used in the interfacial
270 rheology experiments was 20 μm according to the supplier, but light microscopy
271 revealed a broad range of a particle sizes between 1 and 50 μm (data not shown). The
272 ζ-potential of the MCC was therefore not measured because this size range was too
273 large for the NanoSizer. However, many authors [32, 33] report negative values of ζ-
274 potential in the pH range 3 to 7 for all types of MCC produced via acid or alkaline

275 hydrolysis of cellulose, typically in the range of -20 mV to – 30 mV for pH 3 to 7,
276 respectively, depending upon the salt composition of the buffer (which can lead to ion
277 binding). Therefore, it was assumed that the MCC was also negatively charged.
278
279 3.2 Properties and structure of emulsions with WPI + CNCs
280 Figure 2A shows a typical particle size distribution, as determined by static light
281 scattering, for the three emulsions. In absence of CNCs, W1 emulsion had a
282 monomodal droplet size distribution with the majority of droplets being in the range
283 of 0.3–5.0 µm, with an average droplet size (d_{32}) of ~0.45 µm (Table 1), consistent
284 with the TEM image. However, emulsions containing CNCs (W1C1 and W1C3)
285 showed bimodal and trimodal distributions, respectively. In particular, both the
286 emulsions containing CNCs showed a larger proportion of droplets within the 10-100
287 µm size range, with a significant increase in d_{43} > 25 µm (Table 1) as compared to
288 that of W1 emulsion (d_{43} = 2.4 µm) ($p<0.05$). When the W1C1 and W1C3 emulsions
289 were mixed gently with 2% SDS, the distributions reverted to being similar to that of
290 the W1 emulsion (data not shown), which indicated that the emulsions had not
291 coalesced and the several peaks in absence of SDS treatment were most likely due to
292 droplet flocculation [34]. The smaller peak area of the W1C3 emulsion within the
293 0.01-0.1 µm size range logically corresponds to the free CNCs in the continuous
294 phase rather than emulsion droplets and thus, the d_{32} value of the emulsion has been
295 re-calculated removing this peak area from the distribution (Table 1).
296 The morphology of the adsorbed particles was examined by visualisation of
297 the droplet interfaces via negative staining and TEM observations of the emulsions.
298 Figure 2B clearly show CNCs adsorbed on the surface of the W1C1 and W1C3
299 emulsion droplets. However, the secondary surface coverage by clearly discernible

300 CNCs appeared to be rather incomplete in case of W1C1 (Figure 2B). The W1C3
301 emulsion showed more aggregated CNCs closely associated with droplet surfaces
302 forming a rather continuous particulate layer. In both emulsions, the secondary layer
303 of CNCs seemed to be shared between neighbouring emulsion droplets, in agreement
304 with suggestion of droplet flocculation from the size distribution data (Figure 2A).
305 Bridging phenomena of entangling adjacent droplets has been observed with CNCs of
306 this aspect ratio elsewhere [7]. Furthermore, in both the emulsions, a significant
307 degree of particulate network could be observed at the droplet surface (Figure 2B).
308 This might be hypothesized due to CNCs-CNCs aggregation via van der Waals
309 forces, as well as intra- and inter-molecular hydrogen bonds [31] or possible
310 electrostatic complexation between sulphate-bearing CNCs and cationic protein layer
311 at pH. 3 [34]. The size evolution of the CNC aggregates was found to be related to the
312 CNC concentration with more prominent interfacial clusters in W1C3 as compared to
313 W1C1 emulsions, as revealed by the TEM images.

314 The ζ-potential results shows that W1 emulsion was considerably cationic at
315 pH 3 (Table 1), which was expected as whey protein is a zwitterionic polyelectrolyte
316 emulsifier with pI 5.1.With the addition of anionic CNCs (1-3 wt%), the ζ-potential of
317 the whey protein-coated emulsion droplets gradually decreased from +42 to –16 mV.
318 This is obviously most likely due to the increased binding of CNCs to the oppositely
319 charged WPI adsorbed at the oil droplet surface as CNC concentration is increased.
320 This is also consistent with the laser diffraction results showing bridging flocculation
321 in case of W1C1 (Figure 2A), typical with low biopolymeric surface coverage in
322 protein-polysaccharide systems where interactions are net attractive at both the
323 interface and in the bulk phase [35, 36]. In order to confirm this low surface coverage,

324 the degree of secondary surface coverage of CNCs, Γ_{sat} (mg m^{-2}) was calculated using

325 equation (4) [37]:

326 $$\tau_{sat} = \frac{c_{sat} d_{32}}{6\phi} \quad (4)$$

327 where, Φ is the droplet volume fraction (= 0.2) and c_{sat}, the so-called saturation

328 concentration of CNCs i.e. the mass of CNCs adsorbed to cover 95% of the droplet

329 surface per unit volume of emulsion (kg m^{-3}), is given by equation (5) [38]:

330 $$\frac{\zeta_c - \zeta_{sat}}{\zeta_0 - \zeta_{sat}} \approx e^{\left(-\frac{c}{3c_{sat}}\right)} \quad (5)$$

331

332 where, ζ_c is the ζ-potential of emulsion at CNC concentration c, ζ_0 is the ζ-potential

333 without the addition of CNCs (W1 emulsion) and ζ_{sat} is the ζ-potential at c_{sat}. The ζ_{sat}

334 (≈ –55.82 mV) was measured using a control emulsion (3 wt% CNC-coated emulsion

335 droplets, without added WPI). The overall change in droplet ζ-potential at saturation

336 coverage ($\Delta\zeta_{sat} = \zeta_0 - \zeta_{sat}$) was 97.42 mV, which provides an estimate of the amount of

337 charge associated with the adsorbed CNCs molecules upon saturation. For this study,

338 Γ_{sat} calculated using equation (4) was in the range 6–10 mg m^{-2} (Table 1) depending

339 upon the CNC concentration. Such values are lower than the range typically found for

340 surface loads of particles adsorbed to the interfaces [1, 2], but higher than those for

341 adsorbed biopolymer molecules [38]. With the increase of the CNC concentration to 3

342 wt%, the layer at the interface became denser, with 36% higher surface coverage in

343 W1C3 as compared to W1C1 (Table 1).

344

345

346 3.3 Interfacial rheology

347 Interfacial viscosity of adsorbed protein films shows long time dependence due to
348 slow unfolding and cross-linking of proteins and/or changes in interfacial composition
349 due to slow protein desorption. Therefore, for the sake of brevity, we present the
350 measured η_i values at just a 'short' (2 h) and a 'long' (24 h) adsorption time, in Table
351 2. Firstly some measurements were made at the A–W interface at pH 7 to check the
352 correct operation of the instrument and procedures. Although measurements at the
353 A–W interface at first sight might seem not relevant to the O/W emulsions, removing
354 the oil removes complications of interactions between the protein and particles with
355 the oil, which may contain surface active impurities. The value of η_i for β-lg at the
356 A–W interface was seen to increase considerably between 2 and 24 h, from 51 ± 8 to
357 388 ± 72 mN s m^{-1}. Interfacial rheology is very sensitive to the composition and
358 history of the adsorbed film and the reproducibility of values obtained for these
359 conditions are in agreement with previous work [26]. Some experiments were
360 performed with 1 wt% MCC at the A–W interface for interest. Although η_i after 2 h
361 in the presence of 1 wt% MCC was the same (within experimental error) as without
362 cellulose, after 24 h, the MCC apparently caused η_i to decrease to zero (or at least < 2
363 mN s m^{-1}, the limit of detectability with the torsion wire used). This decrease was
364 most likely due to the presence of surface active impurities in the MCC.

365 As mentioned before [28], a significant increase in η_i was shown at the A–W
366 interface on addition of hydrophobically modified cellulose [12]. Additionally, η_i is
367 sensitive to pH, generally reaching a maximum at the isoelectric pH (pI), as long as
368 solubility is maintained. It is seen that η_i (A–W) for β-lg on its own at pH 3 after 2 h
369 was similar to the value at pH 7, but after 24 h, η_i had again apparently decreased to
370 zero, which might be ascribed to greater protein repulsion on the positive side (pH 3)

371 of the protein isoelectric pH (pI, = 5.4) than on the negative (pH 7) side of the pI, or
372 substantial differences in unfolding and cross-linking behaviour at long time, or even
373 acid hydrolysis. Notwithstanding the lack of a completely satisfactory explanation for
374 this decrease, the more important result is that in the presence of 1 wt% MCC this
375 trend was entirely reversed. At pH 3 after 24, β-lg + 1 wt% MCC gave $\eta_i = 130 \pm 9$
376 mN s m^{-1}, the highest value being measured at the A–W interface at this pH (pH 3)
377 and MCC concentration. This is presumably due to the still negatively-charged MCC
378 particles somehow getting trapped in the film of net positively charge β-lg molecules,
379 without the MCC particles necessarily adsorbing to the A–W interface directly.
380 However, the η_i results at the O–W interface at pH 3 did not suggest any significant
381 strengthening of the interfacial film by addition of 1 wt% MCC; in fact all values
382 were zero at 2 or 24 h on addition of 1 wt% MCC. The lower values of η_i may be due
383 to oil molecules or impurities in the oil affecting the surface properties of both the
384 MCC particles and the protein. However, increasing the MCC concentration to 3 wt%
385 apparently swamped any such effects, since once again the adsorbed film was
386 significantly strengthened: the η_i values at 2 and 24 h being 136 and 383 mN s m^{-1},
387 respectively. These results fit in with the much greater accumulation of CNCs
388 apparently observed at the interface of the emulsions with 3 wt% versus 1 wt%
389 cellulose, as observed in calculated surface coverage (Table 1) and TEM images
390 (Figure 2B).
391

392 3.4 Microstructural changes during in vitro gastric digestion

393 As can be observed in Figure 3, the droplet size distribution of W1 emulsion droplets
394 shifted markedly within the first 30 min of gastric digestion, with a considerable
395 proportion of the droplets being in the size range of 10–100 µm. This result is

396 congruent with the visible observation of pronounced creaming and some degree of
397 coalescence, which is also consistent with previous studies [18, 19, 39]. From 30 to
398 120 min, the area of the peak at 10–100 μm remained steady, which might suggest
399 that the proteolysis of the interfacial layer by pepsin progressed relatively rapidly and
400 might be almost complete within the first 30 min.

401 In the case of W1C1 emulsion, the area of the peak at 10 μm increased
402 considerably with parallel decrease of the area of the peak at 1 μm during the first 30
403 min of gastric digestion. During 60–90 min, the area of the peak at 10 μm decreased
404 gradually and area of the peak at 100 μm appeared to increase, suggesting droplet
405 flocculation, which was consistent with the visual creaming. At 120 min, the area of
406 the peak at 100 μm gradually increased to a maximum value indicating that the
407 proteolysis was continuing even at 120 min, which was not the case in case of W1
408 emulsion. In case of W1C3 emulsion, the peak from 0.01–0.1 μm disappeared within
409 the first 30 min, whilst the area of the peak at 1 μm increased. During 30-120 min,
410 digesta mainly consisted of almost equal proportions of two peaks at ~ 1 μm and 10–
411 100 μm, with no visual creaming. Overall, the d_{43} values for both the W1 and W1C1
412 emulsions were markedly higher on completion on 120 min of gastric digestion than
413 those obtained without the addition of pepsin ($p < 0.05$) (Table 1). However, the
414 W1C3 emulsions showed no significant change in d_{43} values during the entire gastric
415 digestion time ($p > 0.05$).

416 The emulsions in the absence and presence of pepsin showed distinctly different
417 arrays of microstructures depending on the concentration of CNC (Figure 4). Prior to
418 addition of pepsin, emulsions showed no clear signs of aggregation. The confocal
419 micrograph of the W1 emulsion illustrates the large-scale microstructural changes
420 observed with droplet flocculation and some degree of coalescence. This might be

421 attributed to weakening of the viscoelastic protein layer at the oil-water interface,
422 after its digestion to lower molecular weight peptides. This probably also explains the
423 substantial loss of surface charge (Table 1), where the ζ-potential fell to near zero (p
424 < 0.05), after digestion, which is in line with previous findings [18, 19, 39].

425 As digestion of W1C1 emulsion progressed, a gradual appearance of well-
426 connected networks of agglomerates was observed, illustrated by the confocal
427 micrograph of the W1C1 emulsions, with no discernible large droplets (Figure 4), in
428 agreement with the laser diffraction results (Table 1). This suggests bridging
429 flocculation via CNC inter-connecting WPI-coated coated droplets rather than their
430 coalescence. Flocculation was considerably more pronounced in W1C1 samples in
431 presence of pepsin (30–120 min) as compared to the some samples in the absence of
432 pepsin (0 min). It therefore appears that the instability of this emulsion under
433 simulated gastric digestion was also associated with the digestive action of the pepsin
434 with significant change in ζ-potential ($p < 0.05$) (Table 1). This suggests that pepsin
435 possibly gained access to the adsorbed protein through the insufficiently complete
436 secondary adsorbed CNC layer, cleaving the WPI proteins and making the residual
437 surface charge of the sulphated CNC particles more prominent. Interestingly, there
438 was still a significant proportion of relatively small droplets that appeared completely
439 coated by CNCs (i.e., droplets apparently stained blue by calcofluor white) (Figure 4).
440 This indicates that the CNCs might form an effective barrier to pepsin attack on some
441 droplets i.e. those that are more completely covered.

442 In the case of W1C3 emulsions, the presence of droplets apparently completely
443 coated with CNCs (i.e. droplets stained blue by calcofluor white) was even more
444 prominent. In fact, a closer look at the micrograph after 30 min of digestion (Figure 4)
445 highlights that the CNCs were not only coating single emulsion droplets but also

446 networking several droplets together within a CNC shell, resembling emulsion
447 microgel particles [40]. This suggests that the attractive forces between CNC and WPI
448 existed not only around individual droplets but also between droplets. Such rigid
449 ‘shells’ might be attributed to a combination of extensive hydrogen-bonding arising
450 from the glucan residues of CNC-CNC [41] as well as the net electrostatic attractive
451 protein-particle interactions [12] as described previously. Even after 120 min of
452 digestion, droplets fully coated by CNCs and not exhibiting significant flocculation or
453 droplet coalescence were observed. Correspondingly, in W1C3, there was no
454 alternation in charge on pepsin digestion (Table 1) ($p > 0.05$), which again suggests
455 that a rigid layer of negatively charged CNC that remains intact and significantly
456 restricts the access of pepsin to the inner-adsorbed protein layer.
457
458 ### 3.5 Hydrolysis of the interfacial protein layer
459 In order to understand the link between the gastric stability of the emulsions and
460 pepsinolysis of the adsorbed protein layer, hydrolysis patterns of the interfacial whey
461 protein (cream phase) from the three emulsions are presented in Figure 5. In either of
462 the protocols (heat treatment or raising pH) that were used to stop the activity of
463 pepsin after gastric digestion, no difference in band patterns was observed (data not
464 shown). In the W1 emulsion, β-lg and α-lactalbumin (α-la) were rapidly digested,
465 with no intact whey proteins remaining after 30 min, as previously reported by Sarkar
466 [18] in β-lg emulsions. The β-lg protein appeared to be digested significantly more
467 slowly in the emulsions containing the WPI + CNC composite layers, particularly
468 during the first 60 min (see the bands at 30 and 60 min (Figure 5A). Interestingly,
469 considerable quantities (40 and 60%) of intact β-lg bands were observed even after
470 120 min of digestion in case of W1C1 and W1C3 emulsions, respectively (Figure

471 5B). Clearly, the electrostatic binding of CNC to WPI at the interface had a prominent
472 effect in diminishing the rate and extent of interfacial proteolysis. Besides the
473 formation of a rigid composite protein-particle layer, electrostatic repulsion between
474 pepsin and CNC layer might have also played an important role, particularly in case
475 of W1C3 emulsions. As the net charge of both pepsin [42] and the original W1C3
476 emulsions (Table 1) were negative at pH 3, the mutual electrostatic repulsion might
477 have contributed to restricted access of the pepsin to the underlying positively charged
478 binding points of the whey protein layer.

479 Golding and Wooster [39] showed that the rate of emulsion digestion was largely
480 controlled by the ability of enzymes to bind to emulsion interfaces, which was
481 determined by emulsion droplet size and interfacial composition. In this study, gastric
482 stability of emulsions was apparently controlled by careful structuring of the
483 interfacial composition. Schematic representations of the possible interactions are
484 given in Figure 6. Although whey protein forms a stable emulsion at pH 3, it could
485 not reduce the digestion rate in gastric conditions due to pepsin-induced rupture of the
486 interface and generation of peptides <10 kDa, which do not provide a sufficiently
487 viscoelastic adsorbed film [18, 19].

488 Binding of CNC to WPI as a secondary layer, probably via attractive electrostatic
489 interactions, produced significant resistance to the breakdown of WPI interfacial layer
490 by pepsin. This is in slight contrast to the results of previous work [12], where neutron
491 reflectivity measurements showed that addition of the non-surface active CNC (0.01
492 wt%) served as steric barrier to physicochemical stresses at pH 4. However, the CNC
493 in the previous study did not give sufficient protection to the interfacial β-lg layer
494 from pepsin attack unless the CNC particles were methylated [12]. This might be
495 attributed to the lower pH (pH 3) and higher (3 wt%) CNC concentrations used in our

496 study, which led to stronger composite formation and a pronounced decrease on the
497 extent and rate of proteolysis.

498 The concentration of CNC and subsequently the secondary surface coverage was
499 found to be a significant factor in dictating the gastric stability of the emulsions.
500 When the concentration of CNC was low (1 wt%), it was insufficient to cover all the
501 droplet surfaces as shown by residual positive charge on the droplets. However, at 3
502 wt%, sufficient coverage of the droplets by a rigid layer of CNC provided steric
503 (mechanical) stabilization. Interestingly, the interfacial viscosity measurements also
504 revealed a large increase in interfacial strength on increasing the MCC concentration
505 from 1 to 3 wt%. Furthermore, the electrostatic repulsion between pepsin and anionic
506 CNCs probably accounted for reduced access of pepsin to the proteinaceous interface.
507 This validates our hypothesis that the presence of CNCs can act as a barrier to pepsin–
508 induced digestion of the WPI at the interface and provide better emulsion gastric
509 stability than oil-in-water emulsions stabilized by WPI alone. However, quantification
510 of network formation of CNCs in the bulk phase versus at the interface require further
511 investigation.

512

513 ## 3 Conclusions

514 The influence of molecular architecture and charge of WPI + CNC composite
515 interfaces on gastric stability has been investigated by means of an array of
516 complimentary physicochemical techniques and microstructural analysis. Our study
517 confirms for the first time that the presence of CNCs decreases the degree and extent
518 of in vitro gastric digestion of the proteinaceous interface by pepsin using SDS-
519 PAGE. This occurs by formation of strong protein-particle composite adsorbed layers
520 at pH 3 exhibiting effective electrostatic and steric repulsion that slows the access of

521 pepsin to the protein interface. At present, we cannot also rule out the possibility of
522 network formation by the CNC in the bulk (continuous) phase and encapsulation of
523 several emulsion droplets together in a rigid CNC shell that also reduces the kinetics
524 and extent of proteolysis. Nevertheless, the present work has uncovered an interesting
525 link between the fundamental interfacial properties of protein-particle composite
526 layers and enhanced gastric stability, which could act in the design of physiologically
527 relevant emulsions. In addition, these findings could have important implications for
528 the design and delivery of lipophilic drugs and bioactive compounds in foods.
529

530 ## Acknowledgements

531 The authors would like to gratefully acknowledge the contributions of Martin Fuller
532 for his technical support in electron microscopy at the Bio-imaging Facility within the
533 Faculty of Biological Sciences. The Zeiss LSM880 microscope used in this work was
534 funded by the Wellcome Trust multi-user equipment award WT104918MA.
535

536 ## References

537 [1] M. Destribats, M. Rouvet, C. Gehin-Delval, C. Schmitt and B.P. Binks,
538 Emulsions stabilised by whey protein microgel particles: towards food-grade
539 Pickering emulsions, Soft Matter, 10 (2014) 6941-6954.

540 [2] A. Sarkar, B. Murray, M. Holmes, R. Ettelaie, A. Abdalla and X. Yang, In vitro
541 digestion of Pickering emulsions stabilized by soft whey protein microgel particles:
542 influence of thermal treatment Soft Matter, 12 (2016) 3558-3569.

543 [3] F. Liu and C.H. Tang, Soy protein nanoparticle aggregates as pickering stabilizers
544 for oil-in-water emulsions, Journal of Agricultural and Food Chemistry, 61 (2013)
545 8888-8898.

546 [4] K. Matsumiya and B.S. Murray, Soybean protein isolate gel particles as foaming
547 and emulsifying agents, Food Hydrocolloids, 60 (2016) 206-215.

548 [5] A. Yusoff and B.S. Murray, Modified starch granules as particle-stabilizers of oil-
549 in-water emulsions, Food Hydrocolloids, 25 (2011) 42-55.

550 [6] M.V. Tzoumaki, T. Moschakis, V. Kiosseoglou and C.G. Biliaderis, Oil-in-water
551 emulsions stabilized by chitin nanocrystal particles, Food Hydrocolloids, 25 (2011)
552 1521-1529.

553 [7] I. Kalashnikova, H. Bizot, P. Bertoncini, B. Cathala and I. Capron, Cellulosic
554 nanorods of various aspect ratios for oil in water Pickering emulsions, Soft Matter, 9
555 (2013) 952-959.

556 [8] E. Dickinson, Biopolymer-based particles as stabilizing agents for emulsions and
557 foams, Food Hydrocolloids.

558 [9] E. Dickinson, Use of nanoparticles and microparticles in the formation and
559 stabilization of food emulsions, Trends in Food Science & Technology, 24 (2012) 4-
560 12.

561 [10] E. Dickinson, Microgels — An alternative colloidal ingredient for stabilization of
562 food emulsions, Trends in Food Science & Technology, 43 (2015) 178-188.

563 [11] M.V. Tzoumaki, T. Moschakis, E. Scholten and C.G. Biliaderis, In vitro lipid
564 digestion of chitin nanocrystal stabilized o/w emulsions, Food & Function, 4 (2013)
565 121-129.

566 [12] N. Scheuble, T. Geue, E.J. Windhab and P. Fischer, Tailored interfacial
567 rheology for gastric stable adsorption layers, Biomacromolecules, 15 (2014) 3139-
568 3145.

569 [13] D.J. McClements and Y. Li, Structured emulsion-based delivery systems:
570 Controlling the digestion and release of lipophilic food components, Advances in
571 Colloid and Interface Science, 159 (2010) 213-228.

572 [14] D.J. McClements, E.A. Decker and Y. Park, Controlling lipid bioavailability
573 through physicochemical and structural approaches, Critical Reviews in Food Science
574 and Nutrition, 49 (2009) 48-67.

575 [15] M. Sjöö, S.C. Emek, T. Hall, M. Rayner and M. Wahlgren, Barrier properties of
576 heat treated starch Pickering emulsions, Journal of Colloid and Interface Science, 450
577 (2015) 182-188.

578 [16] A. Sarkar, J.-M. Juan, E. Kolodziejczyk, S. Acquistapace, L. Donato-Capel and
579 T.J. Wooster, Impact of protein gel porosity on the digestion of lipid emulsions,
580 Journal of Agricultural and Food Chemistry, 63 (2015) 8829-8837.

581 [17] G. Shimoni, C. Shani Levi, S. Levi Tal and U. Lesmes, Emulsions stabilization
582 by lactoferrin nano-particles under in vitro digestion conditions, Food Hydrocolloids,
583 33 (2013) 264-272.

584 [18] A. Sarkar, K.K.T. Goh, R.P. Singh and H. Singh, Behaviour of an oil-in-water
585 emulsion stabilized by β-lactoglobulin in an in vitro gastric model, Food
586 Hydrocolloids, 23 (2009) 1563-1569.

587 [19] H. Singh and A. Sarkar, Behaviour of protein-stabilised emulsions under various
588 physiological conditions, Advances in Colloid and Interface Science, 165 (2011) 47-
589 57.

590 [20] L. Day, M. Golding, M. Xu, J. Keogh, P. Clifton and T.J. Wooster, Tailoring the
591 digestion of structured emulsions using mixed monoglyceride–caseinate interfaces,
592 Food Hydrocolloids, 36 (2014) 151-161.

593 [21] A. Kaboorani and B. Riedl, Surface modification of cellulose nanocrystals
594 (CNC) by a cationic surfactant, Industrial Crops and Products, 65 (2015) 45-55.

595 [22] I. Kalashnikova, H. Bizot, B. Cathala and I. Capron, Modulation of cellulose
596 nanocrystals amphiphilic properties to stabilize oil/water Interface,
597 Biomacromolecules, 13 (2012) 267-275.

598 [23] İ. Gülseren and M. Corredig, Interactions of chitin nanocrystals with β-
599 lactoglobulin at the oil–water interface, studied by drop shape tensiometry, Colloids
600 and Surfaces B: Biointerfaces, 111 (2013) 672-679.

601 [24] Z. Hu, T. Patten, R. Pelton and E.D. Cranston, Synergistic stabilization of
602 emulsions and emulsion gels with water-soluble polymers and cellulose nanocrystals,
603 ACS Sustainable Chemistry & Engineering, 3 (2015) 1023-1031.

604 [25] E. Dickinson, Mixed biopolymers at interfaces: Competitive adsorption and
605 multilayer structures, Food Hydrocolloids, 25 (2011) 1966-1983.

606 [26] B.S. Murray, Interfacial rheology of food emulsifiers and proteins, Current
607 Opinion in Colloid & Interface Science, 7 (2002) 426-431.

608 [27] B.S. Murray, E. Dickinson and Y. Wang, Bubble stability in the presence of oil-
609 in-water emulsion droplets: Influence of surface shear versus dilatational rheology,
610 Food Hydrocolloids, 23 (2009) 1198-1208.

611 [28] B.S. Murray, K. Durga, A. Yusoff and S.D. Stoyanov, Stabilization of foams
612 and emulsions by mixtures of surface active food-grade particles and proteins, Food
613 Hydrocolloids, 25 (2011) 627-638.

614 [29] M. Safouane, D. Langevin and B.P. Binks, Effect of particle hydrophobicity on
615 the properties of silica particle layers at the air−water interface, Langmuir, 23 (2007)
616 11546-11553.

617 [30] T. Hanazawa and B.S. Murray, Effect of oil droplets and their solid/liquid
618 composition on the phase separation of protein–polysaccharide mixtures, Langmuir,
619 29 (2013) 9841-9848.

620 [31] J. George and S.N. Sabapathi, Cellulose nanocrystals: synthesis, functional
621 properties, and applications, Nanotechnology, Science and Applications, 8 (2015) 45-
622 54.

623 [32] P.M. Mosur, Y.M. Chernoberezhskii and A.V. Lorentsson, Electrosurface
624 properties of microcrystalline cellulose dispersions in aqueous solutions of aluminum
625 chloride, nitrate, and sulfate, Colloid Journal, 70 (2008) 462-465.

626 [33] A.N. Zhukov, D.Y. Baturenko, Y.M. Chernoberezhskii and A.V. Lorentsson,
627 Conductivity and electrokinetic potential of microcrystalline cellulose particles in
628 aqueous HCl and NaOH solutions, Colloid Journal, 65 (2003) 310-313.

629 [34] A. Sarkar, K.K.T. Goh and H. Singh, Colloidal stability and interactions of milk-
630 protein-stabilized emulsions in an artificial saliva, Food Hydrocolloids, 23 (2009)
631 1270-1278.

632 [35] K.K.T. Goh, A. Sarkar and H. Singh, Chapter 13 - Milk Protein–Polysaccharide
633 Interactions, in: H. Singh, M. Boland, A. Thompson (Eds.) Milk Proteins (Second
634 edition), Academic Press, San Diego, 2014, pp. 387-419.

635 [36] A. Sarkar and H. Singh, Emulsions and foams stabilised by milk proteins, in:
636 P.L.H. McSweeney, J.A. O'Mahony (Eds.) Advanced Dairy Chemistry, Springer New
637 York, USA, 2016, pp. 133-153.

638 [37] D.J. McClements, Theoretical analysis of factors affecting the formation and
639 stability of multilayered colloidal dispersions, Langmuir, 21 (2005) 9777-9785.

640 [38] D. Guzey and D.J. McClements, Impact of electrostatic interactions on
641 formation and stability of emulsions containing oil droplets coated by *β*-
642 lactoglobulin−pectin complexes, Journal of Agricultural and Food Chemistry, 55
643 (2007) 475-485.

644 [39] M. Golding and T.J. Wooster, The influence of emulsion structure and stability
645 on lipid digestion, Current Opinion in Colloid & Interface Science, 15 (2010) 90-101.

646 [40] O. Torres, B. Murray and A. Sarkar, Emulsion microgel particles: Novel
647 encapsulation strategy for lipophilic molecules, Trends in Food Science &
648 Technology, 55 (2016) 98-108.

649 [41] J. Wang, Q. Cheng, L. Lin and L. Jiang, Synergistic toughening of bioinspired
650 poly(vinyl alcohol)–clay–nanofibrillar cellulose artificial nacre, ACS Nano, 8 (2014)
651 2739-2745.

652 [42] D.R. Davies, The structure and function of the aspartic proteinases, Annual
653 Review of Biophysics and Biophysical Chemistry, 19 (1990) 189-215.